

## Water resource and ecotone transformation in coastal ecosystems

Joseph Park<sup>a,b,\*</sup>, Jed Redwine<sup>a,c</sup>, Troy D. Hill<sup>a,b</sup>, Kevin Kotun<sup>d</sup>



<sup>a</sup> Department of Interior South Florida Natural Resources Center, United States

<sup>b</sup> Physical Resources, United States

<sup>c</sup> Science Communication, United States

<sup>d</sup> U.S. Geological Survey, United States

### ARTICLE INFO

#### Keywords:

Freshwater resource

Mangrove ecotone

Sea level rise

### ABSTRACT

Mangrove marshes are a significant global ecosystem, finely-tuned to contemporary sea level. As sea level rises the mangrove-to-freshwater ecotone reflects underlying groundwater salinity indicating the transformation of freshwater resources into saltwater unsuitable for consumption or agriculture. Hydrological numerical models can predict this dynamic given sufficient environmental detail, however, detailed data is often lacking. Alternatively, agent-based models can predict landscape vegetation changes and the associated fresh-to-saline water transformation based only on landscape surface features. We apply such a model to the southern tip of the Florida peninsula at the nexus of a metropolis and World Heritage wildlife preserve: the Florida Everglades, to predict ecotone dynamics and aquifer water resources in response to warming climate and rising sea level. The model is based on species-specific behaviors for freshwater grasses and salt-tolerant red mangroves with relevance to global mangrove ecosystems.

### 1. Introduction

As climate warms and sea level rises, low-lying coastal ecosystems are among the first to transform with potential for large shifts in ecotones and associated ecosystem services such as sustenance of freshwater resources. These coastal ecotone dynamics reflect landscape changes from the adaptation of terrestrial, estuarine and marine ecosystems in response to perpetual and nonstationary environmental dynamics, and are expressed through a web of complex interactions and feedbacks between biota and environment. Given the inherent nonlinearity and interdependence in these dynamics, one would expect that linear systems analysis may provide unsatisfying results (DeAngelis and Yurek, 2015). As noted by Jiang et al. (2016): “While habitat transitions can be abrupt, modeling the specific drivers of abrupt change between halophytic and glycophytic vegetation is not a simple task. Correlative studies, which dominate the literature, are unlikely to establish ultimate causation for habitat shifts, and do not generate strong predictive capacity for coastal land managers”.

Traditional methods to assess these impacts rely on equation-based models where physical and biological responses are specified with mathematical expressions and/or probabilistic descriptions and interactions (Jorgensen, 1996). Such numerical models have been instrumental in the advancement of our knowledge of coastal systems, however, the expression of emergent behaviors predicated on nonlinear

feedbacks can be problematic in the implementation of equation-based models.

Specific to the nexus of eco-hydrological models, Sivapalan (2018) noted difficulties in accurately quantifying the spatial heterogeneity needed to inform equation-based models, thereby complicating the expression of closure relations at scales of interest. Further, he suggested “instead of specifying exact details of the heterogeneity in our models, we can replace it (without loss of information) with the ecosystem function that they perform”. This perspective aligns with the Earth systems science approach (NASA Advisory Council, 1986) relying on integrative co-evolutionary interactions *in-lieu* of a physical, reductionist approach.

One such alternative is agent-based modeling, where behaviors and feedbacks at the core of the model naturally accommodate nonlinearity and emergence (Grimm and Railsback, 2005). Here, we assess coastal ecotone dynamics with an agent-based model, relying on vegetative transformations in response to sea level driven porewater salinity as a marker for groundwater changes from fresh to saline. Quantification of these changes, both the landscape transformation from freshwater dominated marshes to saltwater dominated estuaries, and the associated changes in freshwater resources are fundamental to the future of inhabited and natural coastal ecosystems.

As an exemplar, we consider the southern tip of the Florida peninsula which is home to both a large metropolitan area and the

\* Corresponding author at: Department of Interior South Florida Natural Resources Center, Homestead, FL 33031, United States.

E-mail address: [Joseph\\_Park@nps.gov](mailto:Joseph_Park@nps.gov) (J. Park).

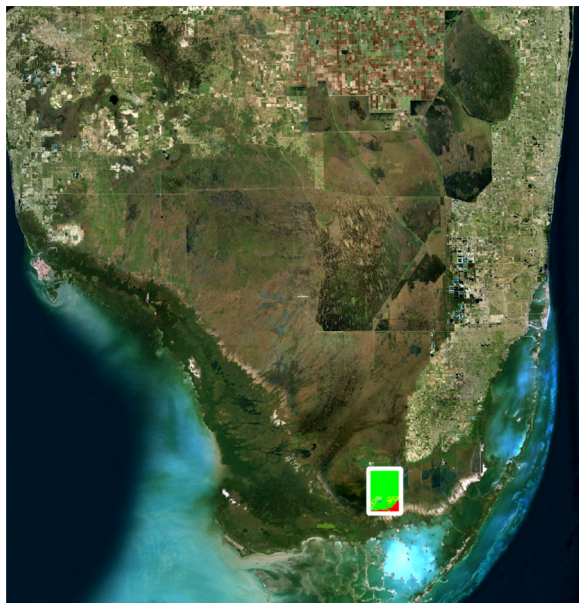


**Fig. 1.** Southern Florida. The east coast is a metropolis of 6.7 million with the South-Dade agricultural area along the southern and western edges. The south central and southwest areas contain the Everglades and Big Cypress National Preserve. The north central area is agricultural and rural. The model domain is shown by the box in the lower center with dimensions 10.2 km × 14.1 km. Dimensions of the overall image are 180 km × 190 km.

Everglades (Fig. 1). The relationship is symbiotic as the Everglades protects and sustains freshwater resources for the natural and urban communities, while concerned citizens and governments are dedicated to preservation and protection of its natural resources. Not only are the Everglades home to spacious freshwater marshes and hardwood hammocks, it includes the largest contiguous fresh-to-saltwater mangrove ecosystem in North America. Such coastal freshwater/mangrove marsh ecosystems are a prominent feature around the globe, with importance as atmospheric carbon sinks, proliferant marine nurseries, and bellwethers of coastal transformation.

## 2. Materials and methods

### 2.1. Analysis domain and data

We estimate the change in vegetation coverage and aquifer freshwater volume under a 14,382 hectare domain spanning a mangrove/freshwater ecotone from 2015 through 2100 in response to a low and high sea level rise trajectory. Fig. 2 shows the model domain with a false color overlay of vegetation in 2015 along the southern peninsula.

Data inputs consist of landscape vegetation coverage obtained from a synthesis of field observations and aerial photography (Ruiz et al., 2017), marsh water levels from the Everglades Depth Estimation Network (EDEN) (Telis et al., 2015), land surface elevations (Fennema et al., 2015), and sea level rise trajectories (Park et al., 2017a). A general description of the modelling framework is provided in the following sections, with a detailed description following the ODD (Overview, Design concepts, and Details) protocol (Grimm et al., 2010) in Appendix A.

### 2.2. Model framework

Agent-based modeling can be viewed as an evolution of cellular automata (Schiff, 2011), finding good success in the analysis of ecosystem complexity and interactions (Grimm and Railsback, 2005). Agent-based models consist of dynamically interacting agents operating in a decentralized, interconnected paradigm accommodating

complexity and emergence. NetLogo is a programmable modeling environment designed to simulate complex phenomena in an agent-based framework (Wilensky, 1999), and is the modeling platform we employ.

NetLogo distinguishes four types of agents: Patches, Turtles, Links, and Observers. Patches represent the world in a grid of cells. Turtles represent agents that operate in the world, interacting with patches and each other. Links provide connections between agents. Observers allow interaction between agents within, and external to the model domain. Our model defines agents for the dominant vegetation species (turtles), agents for the landscape cells (patches), and interactions between agents and the environment.

NetLogo programs conventionally contain `setup` and `go` procedures, the latter being executed in a loop sequencing through agents. Our `setup` procedure loads the timeseries input data, loads GIS shapefiles representing the vegetation map and timeseries mappings, initializes patches with data from the GIS layers, and sprouts turtles on the patches according to the GIS vegetation map species for each cell. The `go` procedure iteratively calls the vegetation agents to assess their vitality, followed by the `propagation` procedure governing species succession in response to environmental feedbacks.

#### 2.2.1. Vitality behaviors

A typical vegetation agent assesses whether the vegetation on a particular patch has been stressed enough to die. For example, *Cladium jamaicense* (sawgrass) contains assessments of water depth and porewater salinity thresholds and durations. Agent vitality behaviors are detailed in Appendix A.4.3.

#### 2.2.2. Succession behaviors

The `propagation` procedure queries each patch devoid of live vegetation, assessing surrounding patches to identify neighboring species. If environmental conditions are conducive for a neighboring species, the species can establish on the vacant patch according to a fitness function shown in Fig. 3. Note that the fitness function is only used to determine vegetation succession, not vitality.

First, a list of vegetation species on the surrounding (8) patches is obtained. A cumulative fitness score is computed for each species by summing the individual fitness scores on a per-species basis. The species with highest cumulative fitness is selected for propagation. However, whether propagation actually occurs is determined by comparison of the species propagation success threshold (i.e. `mangrove-success`, a user-defined parameter) against a randomly selected percentile of a uniform distribution. If succession fails on a particular timestep, there is no penalty on following timesteps, the propagation is run as usual.

Succession behavior rules are detailed in Appendix A.4.3 with water depth and hydroperiod thresholds shown in Table A.4, and succession probabilities listed in Table A.5. Threshold and model parameters values are listed in Table B.1 of Appendix B.

#### 2.2.3. Porewater salinity

The primary ecotone driver from freshwater to salt-tolerant plants is root zone porewater salinity. In the model this is driven by the relative elevation of mean sea level and freshwater depth on the vegetation patch. Since there is a coastal ridge along the northern shore of Florida Bay serving to buffer ocean and estuarine water from the interior, and, since freshwater in the marsh suppresses subterranean saline water in the root zone as expressed by the Ghyben–Herzberg principle, there are two model parameters to calibrate these effects: `msl-offset` and `depth-no-porewater` (see Table B.1 and Fig. B.1).

All patches are initialized to porewater salinity of zero, and have a maximum porewater salinity of 3. This is sufficient since the maximal glycophytic vegetation tolerance is 2 ppt (Table B.1). Patch porewater salinity is then determined by progressive accumulation of porewater salinity for patches with elevation below mean sea level and no standing freshwater.

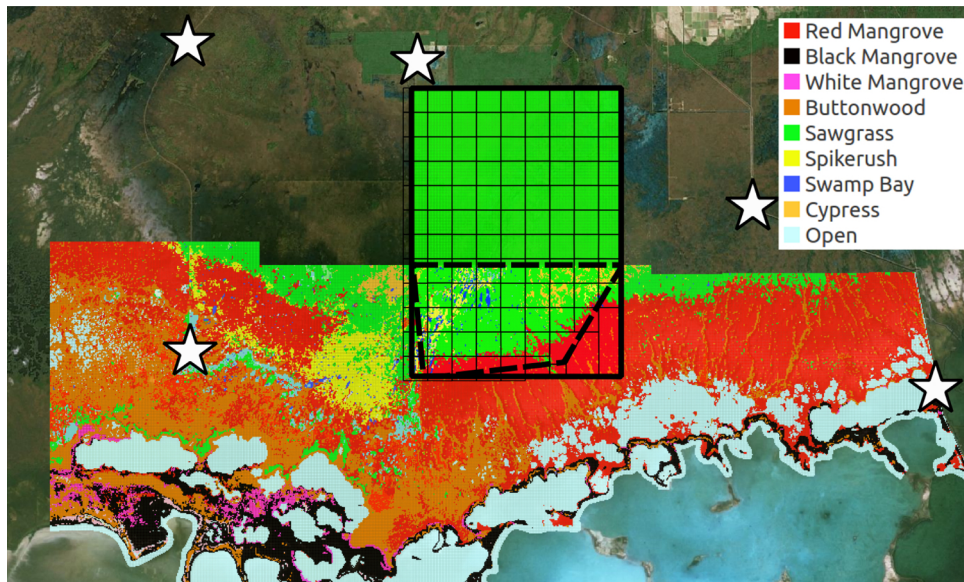


**Fig. 2.** Southern coastal Everglades false color vegetation map. Dashed polygon shows the calibration model domain, rectangle, the future projection domain. The grid defines cells where distinct hydrologic timeseries are applied. Stars indicate locations of wells to estimate aquifer thickness.

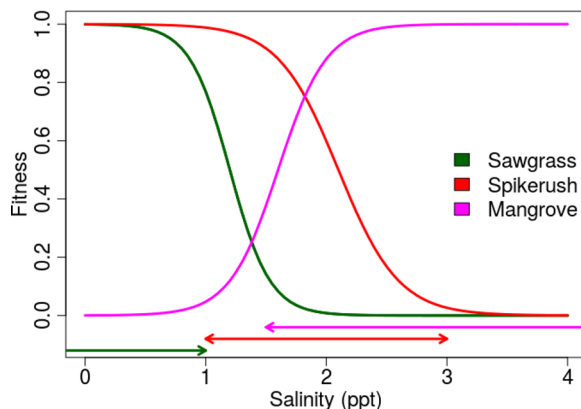


**Fig. 3.** Succession fitness functions for the three dominant species. Horizontal arrows indicate the range of salinities observed by Ross et al. (2000).

Procedurally, all patches with an elevation below mean sea level minus the msl-offset parameter are selected. If these patches have a fresh water depth less than depth-no-porewater, then their porewater salinity is incremented by 1 ppt. If the fresh water depth is greater than depth-no-porewater, the porewater salinity is reset to zero.

### 2.3. Vegetation map

As a component of the Comprehensive Everglades Restoration Plan (CERP), the Department of Interior conducts an extensive vegetation mapping project. The vegetation assessment assigns a landscape characterization code, the *vegetation code*, to 50 m × 50 m patches throughout a region. Vegetation codes derive from a tree of descriptors starting with one of seven overall landscape types, for example Shrubland (S), with additional code elements providing increasing levels of landscape and ecosystem specificity as in Red Mangrove dominant Shrubland (SMr).

Since our model is driven by species behaviors, we assign the dominant species for each landscape code to each of the 50 × 50 m patches. For example, even though a Red Mangrove dominant Shrubland (SMr) may contain other species, the model considers such a patch to be uniformly populated with Red Mangrove. Fig. 2 shows the

southern coastal region vegetation map in Everglades National Park with false color overlay (Ruiz et al., 2017).

### 2.4. Hydrological data

Hydrologic data are informed through the NetLogo time extension, with daily mean water levels provided as timeseries input to patch agents. The link between timeseries and patches is specified in a GIS layer corresponding to the grid shown in Fig. 2. Each model grid cell correspond to 3 × 3 grid blocks from the Everglades Depth Estimation Network (EDEN) (Telis et al., 2015), with the daily water level extracted from the center EDEN cell of the 3 × 3 block.

EDEN observed data are available from 1990 through 2017. Since the calibration model period of record is 1973 through 2015, and the projection model period of record 2015 through 2100, data extrapolation is needed. To model data from 1973 through 1990, we take advantage of strong correlations between marsh water levels across the model domain ( $R^2 = 0.89 \pm 0.09$ ) and estimate missing data with linear regressions from each cell to a long term hydrologic station (P-37) in the central Everglades containing data back to 1973.

Projection model data also leverage strong spatiotemporal correlations to create future projections of stage. First, we compute a single timeseries of daily mean water level across all cells over the observational record (1990–2017) to create a reference timeseries. Second, we compute empirical cumulative distribution functions for each day of the year (year-day, 1–365) over all years of the reference timeseries. Third, we compute linear regressions between the timeseries of each grid cell (1990–2017) and the reference ( $R^2 = 0.95 \pm 0.05$ ). These correlation coefficients will be used to model grid cell water levels from a future projection of the reference timeseries.

Next, the reference timeseries is projected forward in time by sampling from the empirical distribution at the corresponding projected year-day with a Gaussian kernel. Specifically, for a projected year-day, say the first day of the year, the projected value is sampled from the empirical distribution for the first day of the year at a random percentile selected from a normal distribution to produce a projected reference timeseries (2015–2100).

To generate projected timeseries at each cell, the correlation coefficients identified from each cell to the observed reference (1990–2017) are applied to the projected reference. This is tenable since the timeseries are dominated by the yearly hydrologic cycle, and, the flat

topography results in high correlations between model cell hydrologic response as noted above. These projections are purely probabilistic, and do not account for climate change or nonstationarity.

## 2.5. Sea level rise data

Sea level rise trajectories applied to the future projection model are obtained from Park et al. (2017a) corresponding to low (50th percentile) and high (99th percentile) estimates from 2015 through 2100. These estimates are specific to South Florida, and based on a synthesis of tide gauge data, global climate models and expert elicitation, contributions from the Greenland ice sheet, West Antarctic ice sheet, East Antarctic ice sheet, glaciers, thermal expansion, regional ocean dynamics, land water storage and long-term, local, non-climatic factors, such as glacial isostatic adjustment, sediment compaction and tectonics.

As noted in Park et al. (2017a), these projections are comprehensive, but do not include components related to a rapid collapse of Greenland and Antarctic ice sheets. Recent observations suggest that such a collapse is underway (Holland et al., 2015; Wouters et al., 2015), thereby we select the median projection as the low, and the 99th percentile as the high. The sea level rise projections and projected marsh water levels are shown in Fig. 4.

## 2.6. Calibration model

Calibration of agent thresholds and behaviors is achieved by initializing a model spanning the current mangrove/sawgrass ecotone with vegetation coverage observed in 1973 (Rintz and Loope, 1978), which at the time was a purely freshwater landscape as shown in Fig. 5a. The model domain is a grid of 22,990 patches ( $209 \times 110$ ) covering a spatial domain of  $10,450 \times 5500$  m. However, only 17,680 patches are used according to the extent of the 1973 vegetation map.

The model is a four-species model with three freshwater species accounting for 98.8% of the initial vegetation (Sawgrass 92.0%, Spikerush 4.3%, Wax Myrtle 2.5%), and Red mangrove as the saline successor. Other species comprising 1.2% of the initial vegetation are not processed. The model is run forward in time from 1973 to 2015 with parameters adjusted to best fit the observed 2015 landscape vegetation (Fig. 5b). Fit is defined as the percentage of model patches that correspond to the 2015 observed vegetation at the end of the model run. An example applied to two model parameters is shown in Fig. B.1 of Appendix B.

Sea level rise is modeled as a linear function increasing at 3 cm/

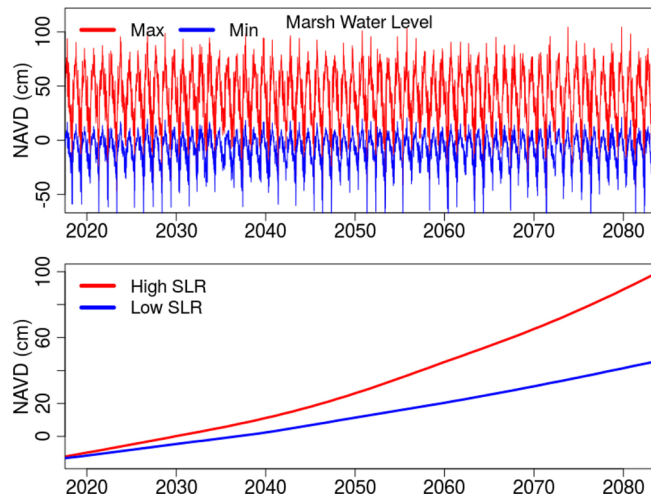


**Fig. 4.** Sea level rise projections (bottom) and projected minimum and maximum marsh water levels (top). Elevations are National Vertical Datum of 1988 (NAVD 88).

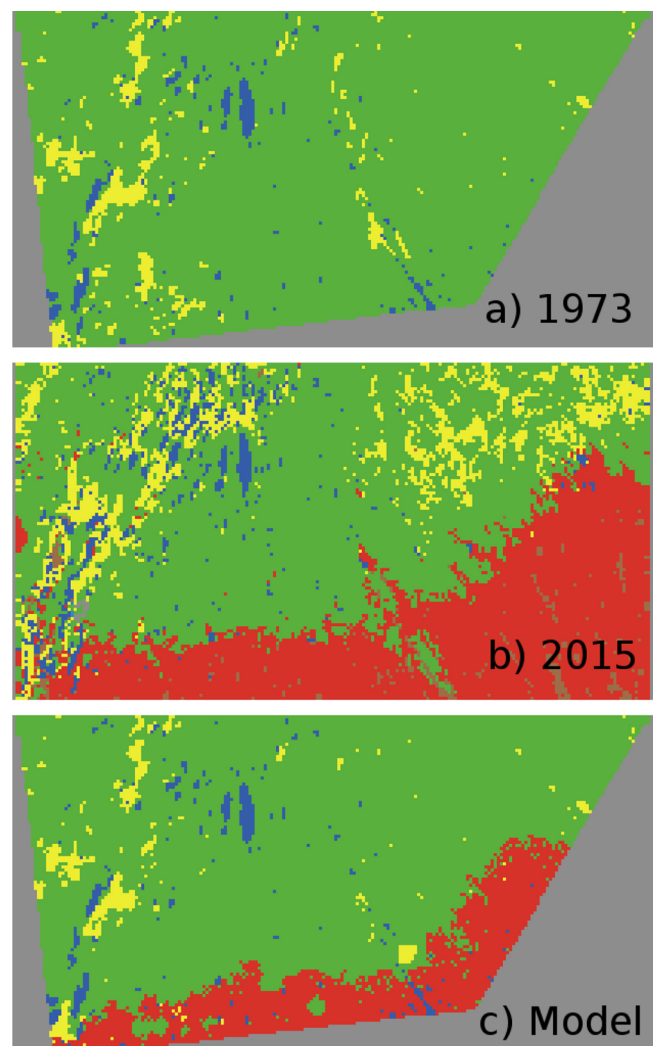


**Fig. 5.** (a) Initial vegetation, 1973. (b) Final vegetation, 2015. (c) Calibration model output at 2015.

decade, corresponding to the mean of observed linear trends at Vaca Key (3.69 mm/yr) and Key West (2.42 mm/yr).

Model output is shown in Fig. 5c. Model parameters are listed in Appendix B, model code and data are available at <https://github.com/SoftwareLiteracyFoundation/Ecotone>.

## 2.7. Projection model

The projection model is a spatial expansion of the calibration model with vegetation initialized from the 2015 vegetation map where available, and with timeseries of marsh stage and sea levels projected from 2015 to 2100. The spatial domain is expanded by 8.6 km to the north and initialized with sawgrass since there is not a vegetation map in this region. The resultant model domain covers 14,382 hectare in a grid of 57,528 patches ( $204 \times 282$ ) 10.2 km wide by 14.1 km tall along the fresh to saline ecotone near Taylor Slough, Everglades National Park (Fig. 2).

The model uses parameters determined by the calibration model (Table B.1), with the addition of one parameter: `msl-open-depth` and three vegetation species, Cypress, Swamp Bay and Buttonwood. The `msl-open-depth` defines a patch depth that when exceeded by mean sea level converts the patch from terrestrial to marine/estuarine. It is set to 70 cm corresponding to maximal freshwater depths.

The three additional species account for 3.5% of the initial species coverage and not considered for propagation. They are assessed for

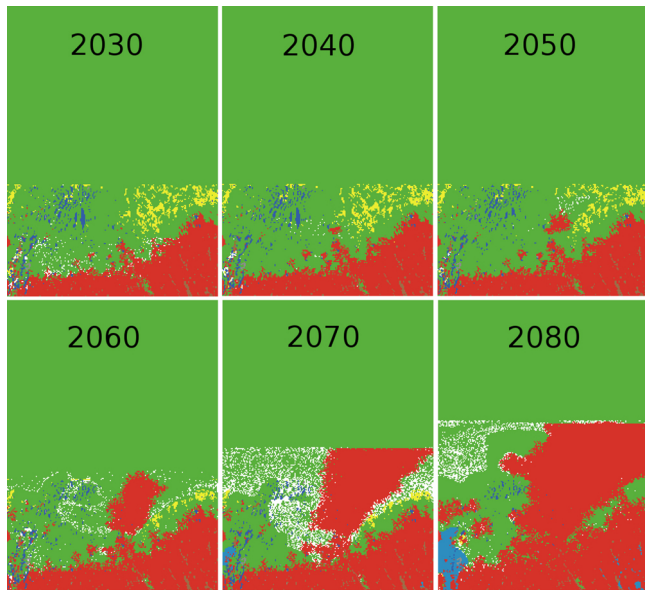


**Fig. 6.** Projected vegetation transformation in response to a low sea level rise trajectory. Vegetation colors correspond to the legend in Fig. 2. White indicates a dead patch.

vitality and can die in response to either MSL exceeding the patch elevation plus `msl-open-depth`, or to salinity exposure in the case of Cypress and Swamp Bay. Their salinity thresholds are set to a maximum salinity of 1 ppt sustained over a period of 30 days.

Model code and data are available at <https://github.com/SoftwareLiteracyFoundation/Ecotone>.

### 3. Results

Predicted landscape transformations under low and high sea level rise trajectories are shown in Figs. 6 and 7 respectively. Under the low sea level rise projection the landscape is relatively unchanged through 2050, with the emergence of a mangrove stand in the south-central model domain. By 2060, the mangrove stand has expanded, and by

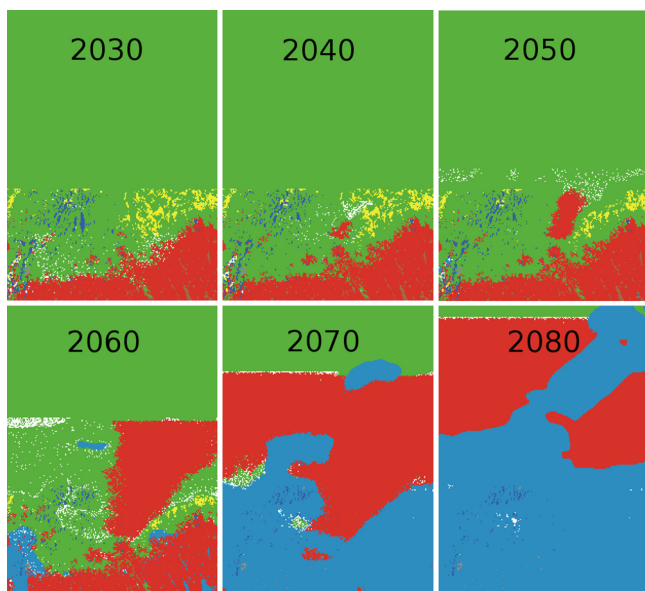


**Fig. 7.** Projected vegetation transformation in response to a high sea level rise trajectory. Vegetation colors correspond to the legend in Fig. 2. White indicates a dead patch.

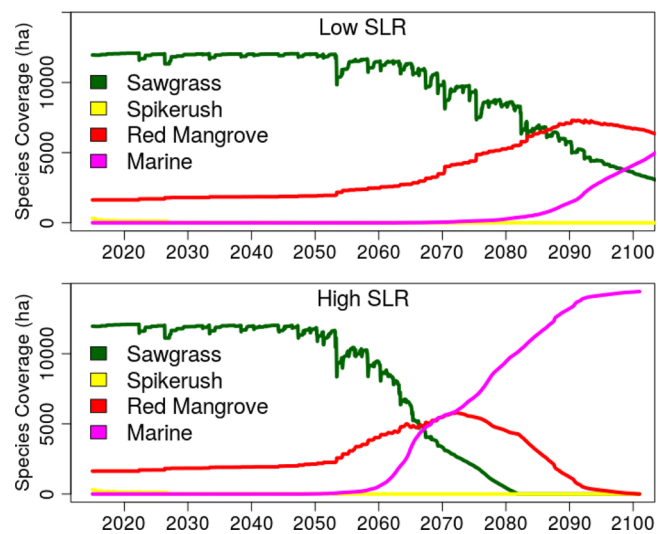


**Fig. 8.** Projection of dominant vegetation coverage and marine (open) area for the low (top) and high (bottom) sea level rise trajectories.

2070 it has nearly engulfed the slightly elevated ridge running from the south central of the domain to the northeast. Landscape elevations are shown in Appendix A.6.1. By 2080 the majority of the landscape seaward of the porewater salinity interface has transformed to mangroves, with the emergence of an open water area in the southwest corner of the domain.

In response to the high sea level rise trajectory, significant change is not forecast through 2040, with the emergence of the south-central mangrove stand by 2050. The ensuing decade is forecast to support the rapid colonization of mangroves along the slightly elevated ridge. By 2070, there has been substantial transformation with open water accounting for a major portion of the domain and a new coastline of mangrove swamp. By 2080 the transformation from predominantly freshwater marsh to marine conditions and mangrove swamp is nearly complete.

Quantification of the areal change in landscape dominant species vegetation cover in response to the two sea level rise forcings is shown in Fig. 8. Under both scenarios the contemporary vegetation distributions remain in equilibrium until 2050, beyond which there is evidence of landscape transformation from freshwater marsh to mangrove marsh and open water.

The physical mechanism behind freshwater to saline-tolerant vegetation transformation is infiltration of root zone porewater salinity. It is also known that as saline water from rising ocean levels infiltrate landward in the surficial aquifer, it does so from the “bottom-up” since saline water is denser than the freshwater (Dausman and Langevin, 2005). From this, we assume that at a point on the landscape where freshwater vegetation has been displaced that the saline water extends to the base of the surficial aquifer.

Given estimates of the surficial aquifer thickness, which here range from approximately 8 to 12 m (Fish and Stewart, 1991), and which are spatially mapped in the model GIS coverage, one can make conservative estimates of the freshwater volume replaced by saline water by using the vegetation coverage as an ecosystem response function. Fig. 9 plots estimates of surficial aquifer volumes under the model domain of fresh and saline water in response to the two sea level rise trajectories assuming a porewater volume fraction of 0.2 (Dausman and Langevin, 2005). Note that this does not require detailed estimates of aquifer properties such as hydraulic conductivity, and that it is not required to estimate landscape vegetation changes.

Model results indicate a transformation from current ecological equilibrium to saltwater dominated starting at 2050. Dynamics of this transition from the freshwater biome perspective are presented in

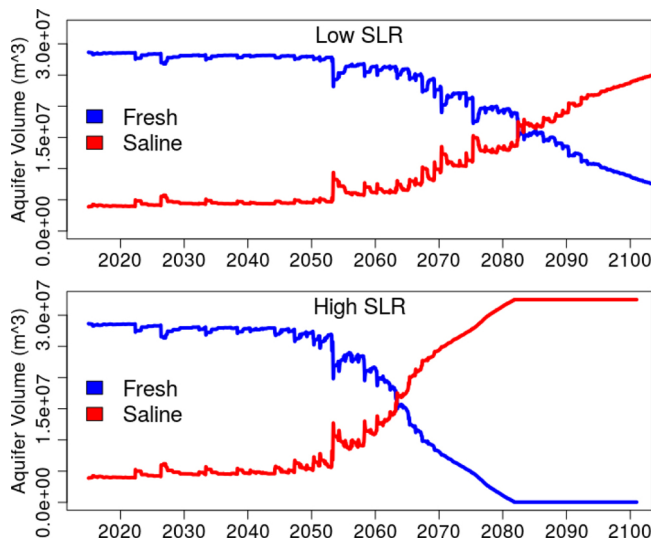


**Fig. 9.** Projection of Fresh and saline water aquifer volumes under the model domain for the low (top) and high (bottom) sea level rise trajectories.

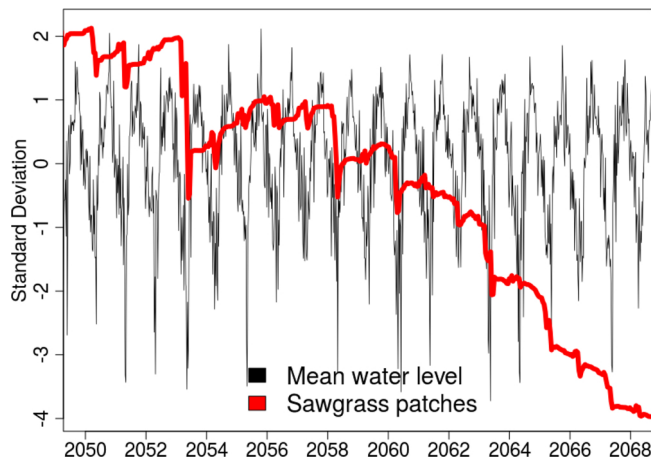


**Fig. 10.** Deviation of spatially-averaged marsh projected water levels compared to scaled sawgrass patch count. Rapid declines in species coverage appear well-correlated with low freshwater elevation events.

**Fig. 10** where deviation of spatially-averaged projected freshwater levels on land are compared with coverage of the dominant freshwater species from 2050 through 2070. Here, we find dynamic responses at two timescales. The long-term decline driven by increasing porewater salinity as ocean levels rise, superimposed with shorter-term yearly or interannual variations exhibiting species proliferation and recovery, with punctuated events of rapid species decline. The rapid declines appear well-correlated with low freshwater elevation events, consistent with observations that drought and dry conditions are a fundamental stressor of freshwater marsh plants, while recovery is indicated during periods without deep water level recession (2054–2058).

#### 4. Discussion

Following the suggestion of Sivapalan (2018) that complex eco-hydrologic domains can be assessed through ecosystem function expressed on the landscape, and the recognition of Jiang et al. (2016) that linear, correlation-based models may not be ideal for capturing ecotone dynamics, we find that an agent based model provides reasonable and compelling estimates for landscape and freshwater resource transformation of coastal marshes in response to sea level rise. The agent based

approach relies on specification of interactions between the environment and species competing on the landscape, rather than highly detailed mappings and assumptions of subterranean aquifer geology and environmental forcings such as rainfall and evapotranspiration. If we were not interested in quantifying the aquifer resource transformation, but simply inferring its areal coverage from the vegetative landscape response, we would not need geologic properties at all.

The model exhibits interspecies competition between fresh and saline tolerant plants, primarily sawgrass (*Cladium jamaicense*) and red mangrove (*Rhizophora mangle*), mediated by root zone porewater salinity determined by elevations of rain-supplied marsh water level, land surface, and sea level. Consistent with known landscape response, elevated porewater salinity denatures freshwater plants during periods of low marsh water level. Open patches are then colonized with fresh or salt tolerant plants depending on environmentally determined fitness functions of surrounding species.

Model results predict continued equilibrium between fresh and saltwater species until 2050, after which there is eventual replacement of freshwater species with salt tolerant ones and fresh groundwater with saline groundwater, ultimately transitioning into new marine habitat. Interestingly, initiation of the transformation is essentially independent of whether sea levels rise along a low or high trajectory, however, the ensuing transformations are quite different as a function of sea level dynamics. This likely reflects a difference between the low and high sea level rise trajectories of 13 cm between 2020 and 2050, but 70 cm between 2050 and 2100. Under a low sea level rise trajectory the model domain transitions from freshwater resource volume of 28.6 million cubic meters in 2015 to 8.7 million cubic meters in 2100, while under a high trajectory the volume decreases to 0 by 2085.

The model also predicts that mangrove establishment at the 2050 threshold is facilitated along a slightly elevated ridge that runs north-east from the lower central model domain. This elevation difference is no more than 14 cm above the surrounding marsh.

The anticipated landscape and aquifer transformation horizons of 2050–2070 are consistent with a purely empirical, independent mechanism and analysis by Park et al. (2017b) assessing transformations in water level exceedances along the coastal ridge in Florida Bay, 8.5 km directly south and seaward of the current mangrove-freshwater ecotone. There, the transformation horizon of 2040–2070 is forecast for the coastal ridge to be continually inundated in response to the same sea level rise trajectories.

As sea level rises, Florida Bay will expand into the Everglades and South Florida establishing new estuarine and marine habitats replacing fresh groundwater along the coastal ecotone. The model predicts that avoidance of extreme low water events and generally higher marsh stage are keys to prolonging viability of freshwater resources, goals expressed in the Comprehensive Everglades Restoration Plan (National Academies of Sciences, 2018).

Further, as shown in the upper right of Fig. 2 and lower right of Fig. 1, the South-Dade agricultural areas are less than 10 km from the model domain. This industry employs more than 20,000 people producing more than \$2.7 billion in annual economic impact (Miami-Dade County Agriculture, 2019), and is predicated on the surficial aquifer as a source of freshwater. Additionally, the Florida Keys Aquaduct Authority extracts potable water for over 70,000 residents from a well-field located less than 5 km from the southern boundary of the agricultural area providing significant concern for saline intrusion (McThenia et al., 2017). Our results suggest that near the end of the century, these areas can start experiencing freshwater resource reduction.

Finally, we note that the model is based on species-specific behaviors in response to root zone porewater salinity with freshwater graminoids and red mangroves the dominant cross-ecotone species. Similar coastal ecotones are found around the globe and can be assessed for water resource transformations using these methods.

## Appendix A. Model overview, design concepts, and details (ODD)

### A.1 Purpose

The models dynamically quantify areal transformation of freshwater marsh into saline estuary in response to dynamic interactions between freshwater depth and root zone porewater salinity driven by sea level. Landscape vegetation changes are used as indicators of surficial groundwater salinization, allowing estimates of changes fresh-to-saline water volumes in the surficial aquifer.

### A.2 Entities, state variables, and scales

#### A.2.1 Agents

Model agents consist of plant species (NetLogo turtles) and landscape grid cells (NetLogo patches). Plant species agents are listed in [Table A.1](#) with initial coverage percentages listed in [Tables A.8 and A.9](#). The Open Water agent is an end-point transformation for the other species.

State variables of the plant and grid cell agents are listed in [Tables A.2 and A.3](#) respectively.

**Table A.1**  
Model agents.

Species	Calibration model	Projection model
Red Mangrove	X	X
Sawgrass	X	X
Spikerush	X	X
Buttonwood		X
Cypress		X
Swamp Bay		X
Wax Myrtle	X	
Open Water	X	X

**Table A.2**  
Plant species variables.

Variable	Unit	Description
species		Species name
salinity_max	ppt	Maximum tolerable salinity
salinity_max_days	days	Maximum duration of tolerable salinity

**Table A.3**  
Landscape cell variables.

Variable	Unit	Description
depth	cm	Water depth
days_wet	days	Hydroperiod
days_dry	days	Consecutive days dry land surface
salinity	ppt	Salinity from timeseries (optional)
porewater_salinity	ppt	Root zone porewater salinity
salinity_threshold	ppt	Salinity the current cell species can tolerate
salinity_days	days	Consecutive days with salinity above threshold
cell_ID		Cell ID from vegetation map
elevation	cm	Ground elevation (NAVD88)
reason_died		Reason species died
day_died	date	Date the species died
stage_gauge		Gauge for water stage timeseries
aquifer_m	m	Aquifer thickness
species_init		Initial species

**Table A.4**

Vitality behaviors. When the condition variable exceeds the threshold, the plant dies. Thresholds are expressed as the NetLogo model variable name (Table B.1).

Species	Condition
Red Mangrove	MSL > patch elevation + 80 cm
Sawgrass	depth > sawgrass-depth-max
Sawgrass	days above salinity threshold > sawgrass-salinity-threshold
Spikerush	depth > spikerush-depth-max
Spikerush	days dry > spikerush-days-dry
Spikerush	days above salinity threshold > spikerush-salinity-threshold
Wax Myrtle	depth > wax-myrtle-depth-max
Wax Myrtle	days wet > wax-myrtle-days-wet
Wax Myrtle	days above salinity threshold > wax-myrtle-salinity-threshold

**Table A.5**

Succession failure conditions. Model parameter values are shown in Table B.1.

Species	Condition
Sawgrass	sawgrass-success < uniform percentile
Sawgrass	depth > sawgrass-depth-min
Spikerush	spikerush-success < uniform percentile
Spikerush	days wet < spikerush-days-wet
Mangrove	mangrove-success < uniform percentile
Mangrove	depth > depth-propagule

**Table A.6**

Plant species agent environmental sensing variables.

Species	Variable	Description
Spikerush	MSL	Mean sea level elevation
	depth	Landscape water depth
	days_wet	Consecutive days with inundation
	salinity_days	Consecutive days above salinity threshold
	days_dry	Consecutive days without inundation
	salinity_days	Consecutive days above salinity threshold
Red Mangrove	MSL	Mean sea level elevation
Cypress	salinity_days	Consecutive days above salinity threshold
Swamp Bay	MSL	Mean sea level elevation
Buttonwood	salinity_days	Consecutive days above salinity threshold
Wax Myrtle	MSL	Mean sea level elevation
	days_wet	Consecutive days with inundation
	depth	Landscape water depth

**Table A.7**

Hydroperiod modulation.

Species	Variable	Min	Max	Modulation
Sawgrass	days-wet	0	365	N(0,15) days
Wax Myrtle	days-wet	0	1000	N(0,15) days
Spikerush	days-dry	0	1000	N(0,10) days

**Table A.8**  
Initial species of the calibration model.

Species	Count	Percent
Sawgrass	16256	92.0
Spikerush	758	4.3
Wax Myrtle	441	2.5
Cypress	125	0.7
Red Mangrove	0	0.0

**Table A.9**  
Initial species of the projection model.

Species	Count	Percent
Sawgrass	47835	83.1
Red Mangrove	6523	11.3
Spikerush	1258	2.1
Cypress	1070	1.8
Swamp Bay	671	1.1
Buttonwood	395	0.6

**Table A.10**  
Data input files.

Model Variable	File type	Purpose
Stage.data	csv	Marsh water level
MeanSeaLevel.data	csv	Mean sea level
VegMap	shp	Species to cell mapping, cell elevation
GaugeZones	shp	EDEN data to cell mapping

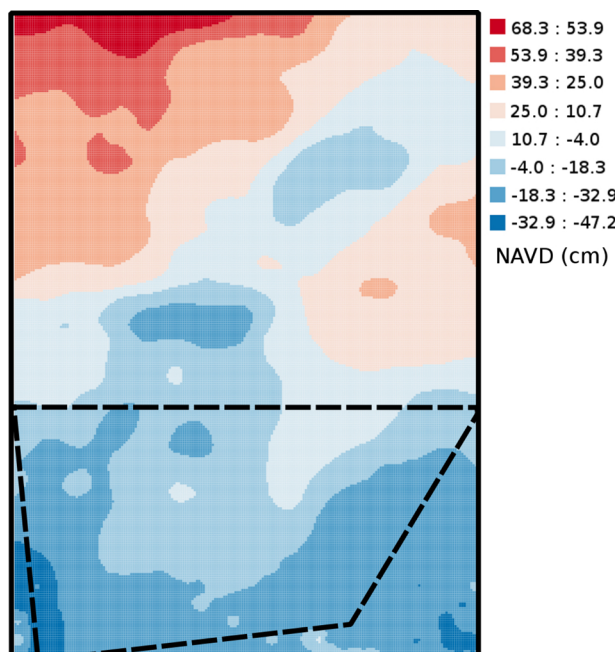


**Fig. A.1.** Elevation map of the model domain. Dashed polygon is the calibration model domain.

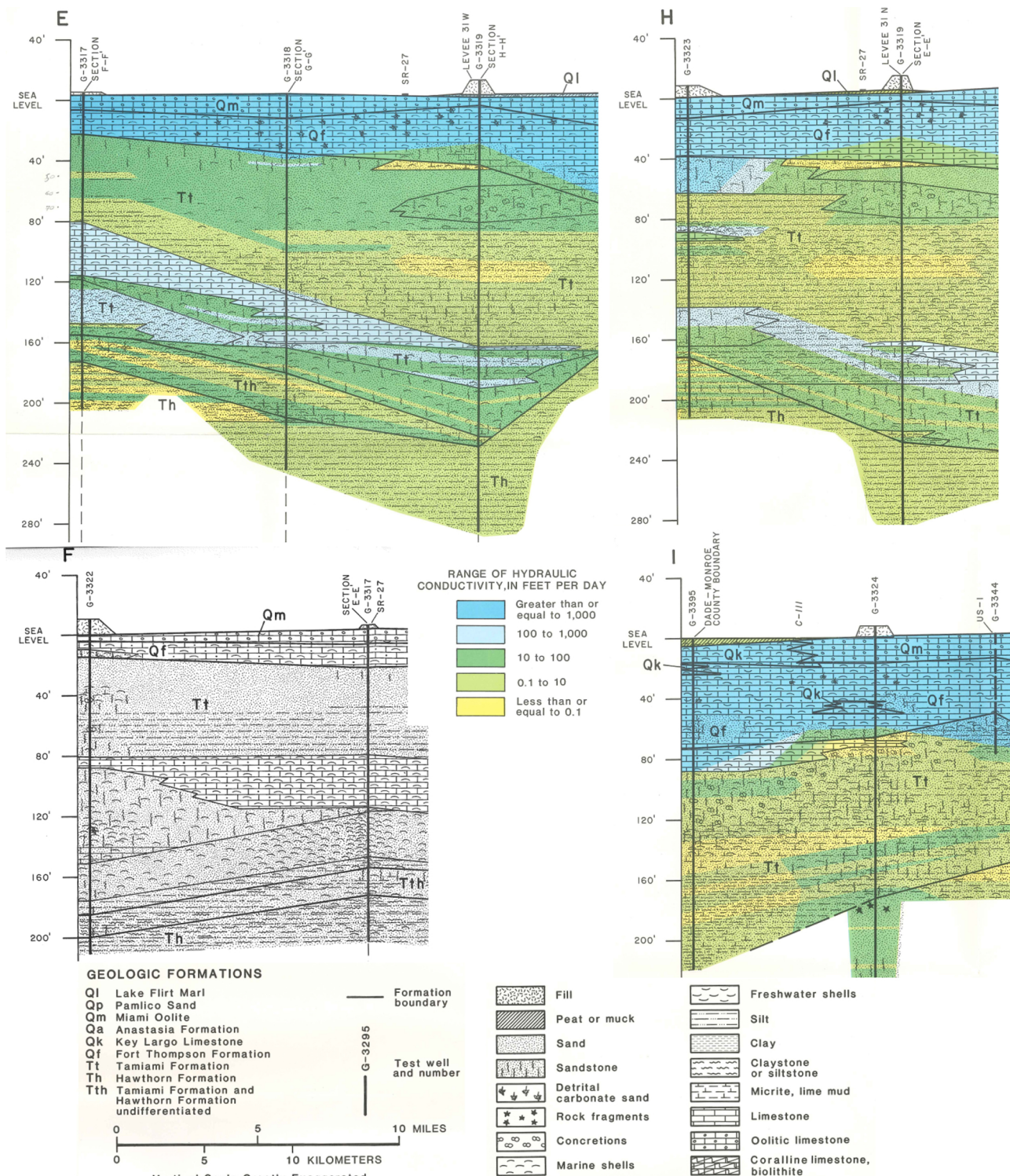


Fig. A.2. Geologic cross sections from United States Geological Service wells (Fish and Stewart, 1991).

#### A.2.2 Spatial units

Landscape grid cells correspond to the  $50\text{ m} \times 50\text{ m}$  spatial discretisation of the vegetation map developed by Ruiz et al. (2017). The calibration model domain is a grid of 22,990 patches ( $209 \times 110$ ) covering a spatial domain of  $10.4 \times 5.5\text{ km}$ . The projection model covers 14,382 ha in a grid of 57,528 patches ( $204 \times 282$ )  $10.2\text{ km}$  wide by  $14.1\text{ km}$  tall.

### A.2.3 Environment

The model environment consists of three primary variables: land surface elevation, water depth in relation to land surface, and sea level elevation. Land surface elevation is assigned to each model grid cell from a GIS layer based on the work of Fennema et al. (2015) as described in Appendix A.6.

Daily water elevations are obtained from the Everglades Depth Estimation Network (EDEN) (Telis et al., 2015) and mapped to landscape cells through a GIS layer and the cell `stage_gauge` variable. The GIS layer (specified in Appendix A.6) assigns to each cell the name of an EDEN cell from which the water level timeseries are applied. A csv file of the EDEN timeseries data is dynamically accessed to retrieve the corresponding water elevation at each timestep.

Sea level elevations are obtained from timeseries of projected sea levels in Florida Bay by Park et al. (2017b).

### A.3 Process overview and scheduling

Model timesteps are discretely updated with a user-adjustable variable `days-per-tick` with a default value of 15 days. Since input data are available in daily increments the model timestep can be any period of days. The appropriate data is selected according to the specific date of a model timestep.

The `go` function schedules agent and data process execution at each timestep as shown here and described in detail in Appendix A.7.

```
; Load mean sea level for this timestep
set MSL time:ts-get MeanSeaLevel.data date SLR-scenario
update-patch-depth-salinity
; Process species agentsets for environmental impact, vitality
go-sawgrass
go-spikerush
go-red-mangrove
go-cypress
go-swamp-bay
go-buttonwood
; Process dead patches for succession
go-propagation
tick; increment time by days-per-tick
```

## A.4 Design concepts

### A.4.1 Basic principles

The models assume a fundamental driver of ecotone dynamics between freshwater marsh and saline estuary is root zone porewater salinity, and that this salinity is mediated by dynamic balance between sea level elevation, landscape cell elevation and freshwater that may be present on the cell. Species-specific tolerances to root zone salinity, hydroperiod and depth dictate plant vitality and death, while porewater salinity determines species-specific fitness for succession.

### A.4.2 Emergence

The model is fundamentally one of interspecies competition driven by root zone salinity. Primal complexities arise from the nonlinear nature of landscape freshwater depth and randomness of plant death and succession. Therefore, we do not expect behavioral emergence from interagent interactions.

### A.4.3 Adaptation

Vegetation agents do not internally adapt or change behaviors, but they do respond to environmental changes. These behaviors are governed by salinity thresholds prescribed by the logistic functions shown in Fig. 3, water depth and hydroperiod thresholds shown in Table A.4, and succession probabilities listed in Table A.5.

For example, based on observational data as expressed in Fig. 3, sawgrass can tolerate salinities near 1 ppt while for spikerush 2 ppt can be tolerated. The depth parameter relates a water depth on the patch beyond which the plant is unable to transpire or its cellular structure is compromised, days wet represents the continuous hydroperiod that the plant can tolerate resulting in decomposition of roots, transpiration limits, or cellular compromise. Days dry represents the tolerable period of time with no available water in the root zone resulting in desiccation.

Threshold and model parameters values are listed in Table B.1 of Appendix B.

As noted in Section 2.2.2, when empty cells are evaluated for species succession the surrounding species with the highest cumulative fitness is selected for propagation. However, whether propagation actually occurs is determined by comparison of the species propagation success threshold as listed in Table A.5 to a uniform random variate.

### A.4.4 Objectives

As noted in the preceding section, agents do not engage in internal behavior or objective (fitness) adaptation, however, their objectives are responsive to the environment as detailed in the preceding section.

#### A.4.5 Learning

As noted in the preceding section, agents do not alter or dynamically change their adaptive traits, rather they respond to the environment.

#### A.4.6 Prediction

Agents do not project or anticipate future states.

#### A.4.7 Sensing

Environmental state variables that individuals are assumed to sense and consider in their decisions are listed in [Table A.6](#).

#### A.4.8 Interaction

Interactions exist between the landscape cell (NetLogo patch) and the vegetation agent (NetLogo turtle) on the cell. The cell maintains information regarding water depth, hydroperiod, and porewater salinity. Vegetation agents process this state information to determine vitality and fitness. There are no interagent interactions between vegetation agents.

The only feedback in the model acts within landscape cells to determine porewater salinity. Porewater salinity is forced by the elevation of mean sea level in relation to the elevation of the cell (land surface), but can be mediated by the presence of adequate freshwater depth on the cell as described [Appendix A.7.1](#).

#### A.4.9 Stochasticity

Evaluation of environmental variables `days-wet` and `days-dry` in plant vitality behaviors are randomly modulated with a Gaussian kernel to simulate individual plant tolerances. Specifically, when a patch hydroperiod is processed, the physically simulated value is shifted by the number of days according to a normal distribution specified in [Table A.7](#).

Vegetation succession behaviors are also probabilistically influenced as described in [Section 2.2.2](#) and [Appendix A.4.3](#).

#### A.4.10 Collectives

The models use agent collectives (NetLogo agentsets) internally to avoid redundant operations. For example, collectives of cells with specific species, or which have transformed to open water. There are no collective behaviors associated with these collectives.

#### A.4.11 Observation

The number of patches of sawgrass and red mangrove are the primary observational variables of the models.

#### A.5 Initialization

Each cell in the model is initialized with a vegetation species specified from a vegetation map. The calibration model uses the 1973 vegetation map of [Rintz and Loope \(1978\)](#), while the prediction model uses the 2015 map of [Ruiz et al. \(2017\)](#). Timeseries data of water depth and mean sea level elevation are initialized according to the user-specified `start-date` variable. [Appendix A.6](#) details the input and initialization data.

Initial species compositions for the calibration and projection models are shown in [Tables A.8](#) and [A.9](#) respectively.

#### A.6 Input data

[Table A.10](#) lists the input files and associated variable names used in the models. All timeseries data have daily resolution, and extend over the model period of record with no repeated data.

Sea level rise and marsh water level extrema are shown in [Fig. 4](#), cell elevations are shown in [Fig. A.1](#).

#### A.6.1 Elevation data

The interplay between freshwater depths, mean sea level and porewater salinity are largely determined by landscape elevation. [Fig. A.1](#) shows the model domain elevation indicating a southwest to northeast channel known locally as Taylor Slough. There is also a small ridge south of Taylor Slough running southwest to northeast. Model simulations suggest that this ridge will provide an initial stand for red mangroves as sea levels rise.

#### A.6.2 Aquifer geological data

Aquifer thickness is inferred from United States Geological Service wells and geologic cross-sections shown in [Fig. A.2](#).

#### A.7 Submodels

Model processes specified [Appendix A.3](#) are detailed here.

##### A.7.1 Update patch depth salinity

The procedure `update-patch-depth-salinity` executes these steps at each timestep:

- 1 Set depth on all cells.
- 2 Accumulate hydroperiod (`days_wet`, `days_dry`) for all cells.
- 3 Identify cells with elevation below mean sea level into `msl_patches`.

- 4 Identify `msl_patches` in coastal zone within 1.5 km of mangrove ecotone.
- 5 Identify `msl_patches` cells with freshwater depth less than `depth-no-porewater` into `porewater_patches`.
- 6 Increment `porewater_salinity` of `porewater_patches`.
- 7 Identify `msl_patches` with freshwater depth greater than `depth-no-porewater` into `no_porewater_patches`.
- 8 Reset `porewater_salinity` to zero for `no_porewater_patches`.
- 9 For `msl_patches`:
  - (a) Update cell salinity.
  - (b) Accumulate number of days above `salinity_threshold` into `salinity_days`.

#### A.7.2 Plant vitalities

Each plant species/agent is assessed for vitality based on the current and accumulated environmental conditions in the `go-species` procedures. These procedures follow a common set of steps based on the specific tolerances for each species as identified Appendix A.4.3.

- 1 Identify cells with living species (i.e. sawgrass).
- 2 If needed, apply Gaussian offsets to hydroperiod variables to emulate individual plant tolerances as described Appendix A.4.9.
- 3 Determine if the plants die by applying the environmental conditions and species thresholds described Appendix A.4.3.
- 4 If plant has died, record the model time and reason for death.
- 5 If plant has died, remove the cell from the species cell collection.

#### A.7.3 Succession

The `go-propagation` procedure processes patches with no living plants for succession.

- 1 Identify species on surrounding (8) cells into `neighbor_species`.
- 2 Accumulate the porewater salinity mediated fitness score (Fig. 3) for each species in `neighbor_species`.
- 3 If there is a tie in fitness, randomly (50% uniform deviate) select one of the species and reduce its fitness by 0.1.
- 4 Identify the species with maximum cumulative fitness.
- 5 Apply the species-specific propagation threshold against a uniform random variate to decide if the selected species will actually propagate as described in Section 2.2.2.
- 6 If a species establishes on the cell, set the species-specific environmental tolerances into the cell agent variables.

## Appendix B. Calibration model

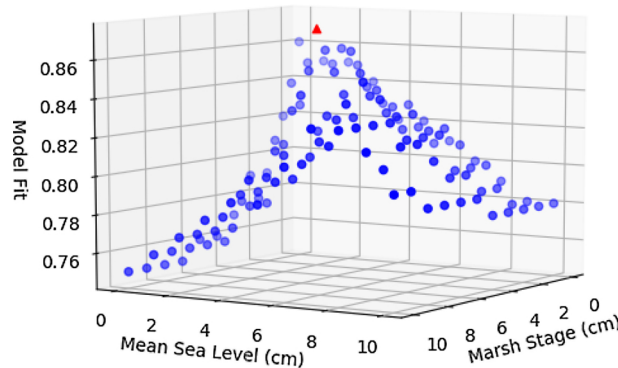
Calibration model parameters are shown in Table B.1.

Fig. B.1 plots model calibration fit in response to `msl-offset` and `depth-no-porewater` finding optimal values of 2 cm for both parameters. Fit is defined as the percentage of model patches that correspond to the 2015 observed vegetation at the end of the model run.

The NetLogo user interface for the calibration model is shown in Fig. B.2.

**Table B.1**  
Calibration model parameters.

Parameter	Value	Description
<code>msl-offset</code>	2 cm	Elevation below Mean Sea Level
<code>depth-no-porewater</code>	2 cm	Marsh water depth min for fresh root zone
<code>mangrove-success</code>	33%	Probability of propagation success
<code>depth-propagule</code>	7 cm	Maximum depth for propagule establishment
<code>sawgrass-success</code>	33%	Probability of propagation success
<code>sawgrass-depth-min</code>	20 cm	Maximum depth for propagation
<code>sawgrass-depth-max</code>	180 cm	Maximum depth for survival
<code>sawgrass-salinity-threshold</code>	1	Salinity threshold for survival
<code>sawgrass-salt-days</code>	20	Maximum number of days above threshold
<code>spikerush-success</code>	33%	Probability of propagation success
<code>spikerush-days-wet</code>	730	Hydroperiod for propagation
<code>spikerush-depth-max</code>	80 cm	Maximum depth for survival
<code>spikerush-days-dry</code>	170 cm	Maximum days dry for survival
<code>spikerush-salinity-threshold</code>	2	Salinity threshold for survival
<code>spikerush-salt-days</code>	20	Maximum number of days above threshold
<code>wax-myrtle-depth-max</code>	180 cm	Maximum depth for survival
<code>wax-myrtle-days-wet</code>	370	Maximum hydroperiod for survival



**Fig. B.1.** Model fit as a function of mean sea level offset and marsh stage offset that control porewater salinity.

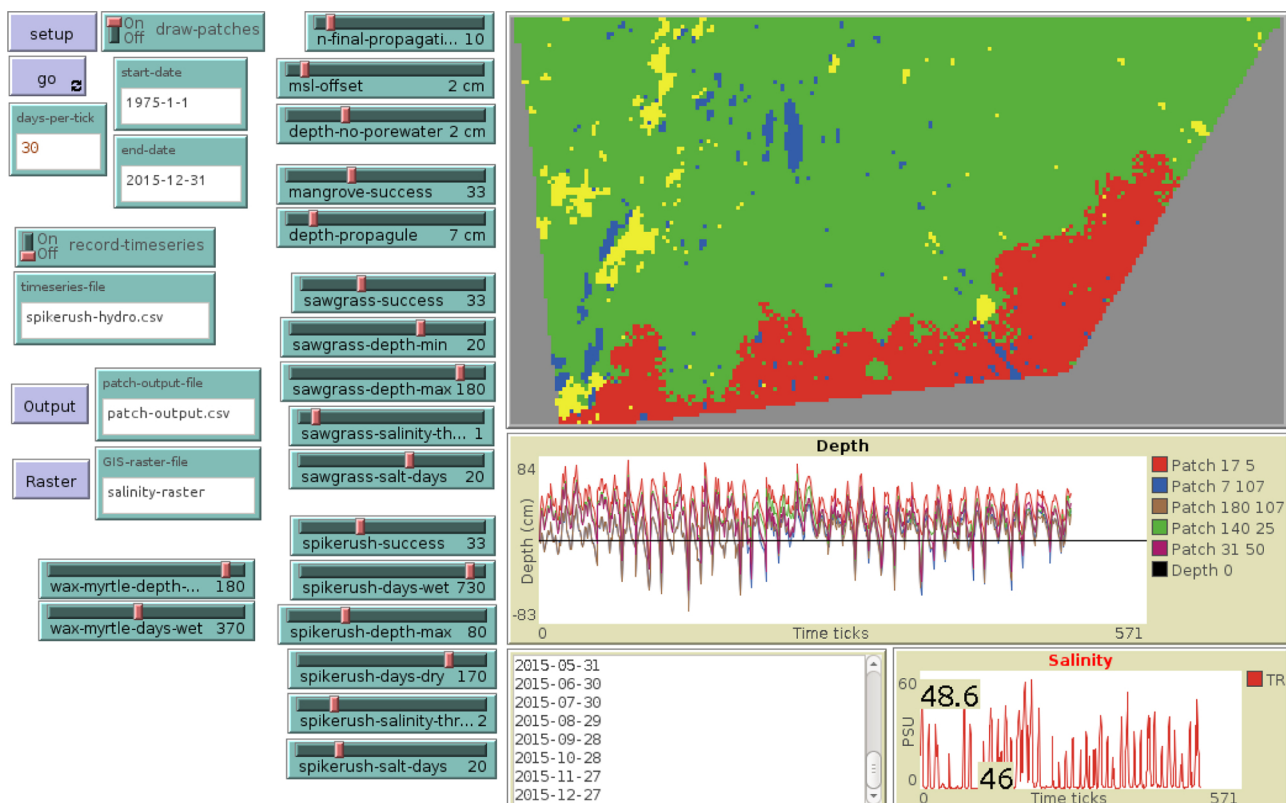


**Fig. B.2.** NetLogo model user interface for the calibration model.

### Appendix C. Projection model

The projection model uses the same parameters as the Calibration model (Table B.1). The NetLogo user interface for the projection model is shown in Fig. C.1.

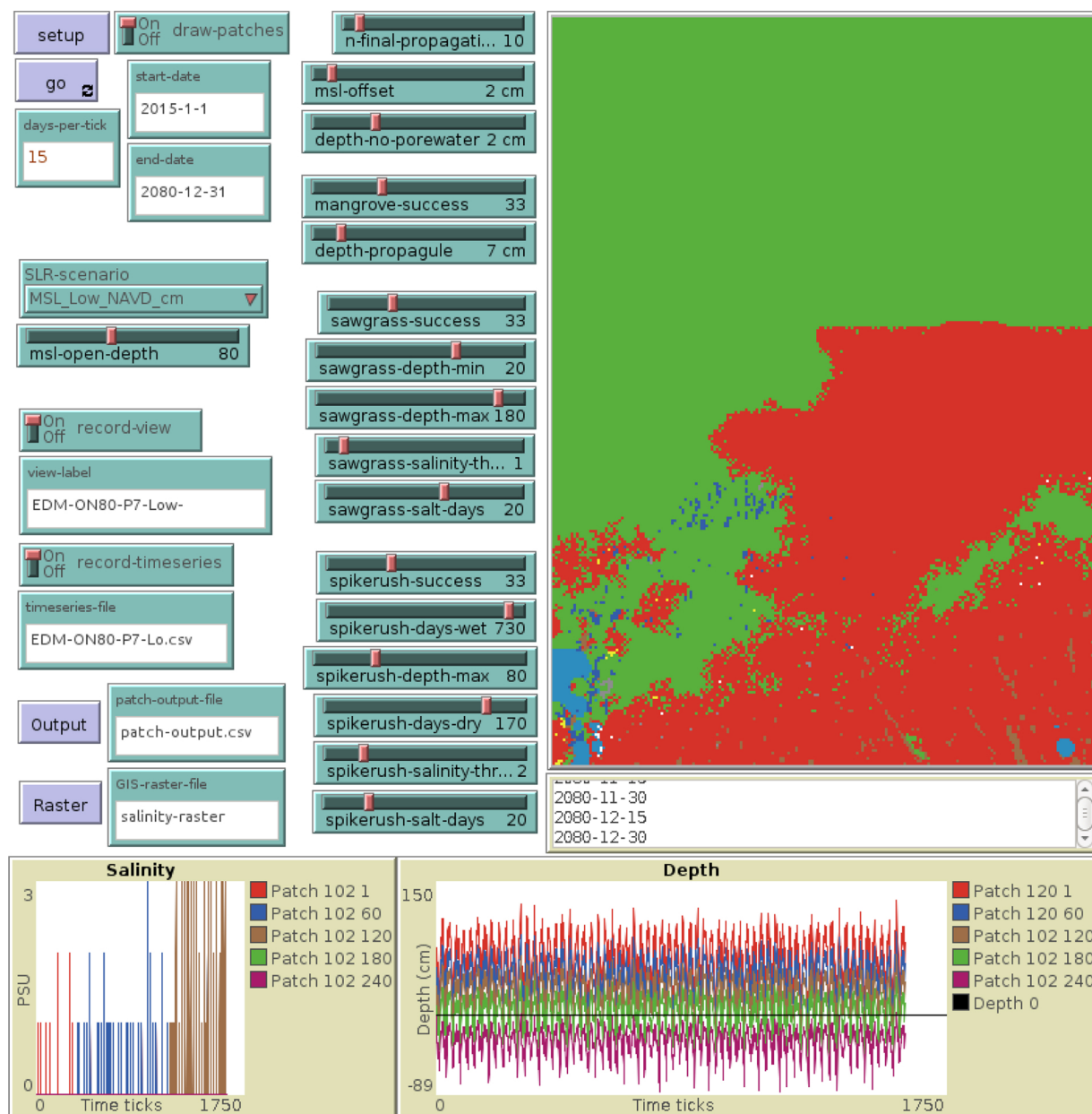
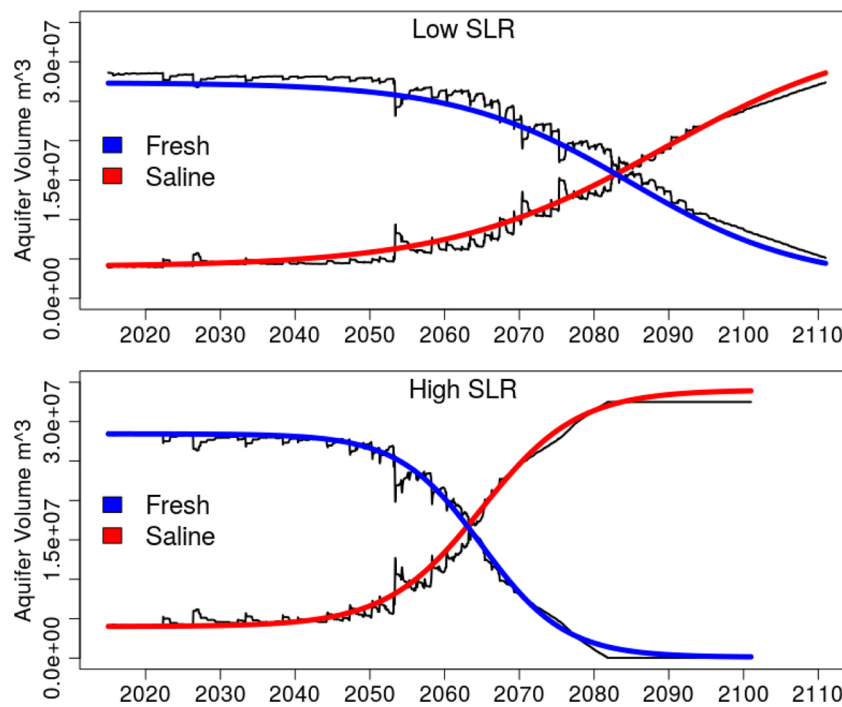


Fig. C.1. NetLogo model user interface for the projection model.

## Appendix D. Aquifer volume fit

A generalized logistic function  $V = V_0 + \frac{V_{max}}{1 + \exp(-a(x - x_0))}$  is fit to the aquifer volume estimates with a Nelder–Mead optimization (Nelder and Mead, 1965) as shown in Fig. D.1 and Table D.1.



**Fig. D.1.** Generalized logistic function fits to the estimated aquifer water volumes.

**Table D.1**

Best fit parameters for generalized logistic function  $V = V_0 + \frac{V_{max}}{1 + \exp(-a(x - x_0))}$  fit to estimated aquifer water volumes.

SLR	Water	a	$V_{max}$	$V_0$	$x_0$
Low	Salt	0.0001907	29999684	4011159	2089-04-04
Low	Fresh	-0.0002369	25303766	2051779	2084-11-14
High	Salt	0.0004285	29999999	4010603	2064-12-31
High	Fresh	-0.0004918	28322591	117512	2064-12-31

## References

- Dausman, A., Langevin, C.D., 2005. Movement of the saltwater interface in the surficial aquifer system in response to hydrologic stresses and water-management practices. USGS Scientific Investigations Report 2004-5256, Broward County, Florida. <http://pubs.usgs.gov/sir/2004/5256/>.
- DeAngelis, D.L., Yurek, S., 2015. Equation-free modeling unravels the behavior of complex ecological systems. Proc. Natl. Acad. Sci. U. S. A. 112 (13), 3856–3857. <https://doi.org/10.1073/pnas.1503154112>.
- Fish, J., Stewart, M., 1991. Hydrogeology of the Surficial Aquifer System, Dade County, Florida, Water-Resources Investigations Report 90-4108. U.S. Geological Survey. <https://pubs.er.usgs.gov/publication/wri904108>.
- Fennema, R., James, F., Bhatt, T., Mullins, T., Alarcon, C., 2015. EVER Elevation (version 1): A Multi-sourced Digital Elevation Model for Everglades National Park. National Park Service, Everglades National Park, Homestead, FL, USA July 10, 2015.
- Grimm, V., Railsback, S.F., 2005. Individual-Based Modeling and Ecology. Princeton University Press, Princeton, NJ.
- Grimm, V., Berger, U., DeAngelis, D., Polhill, J., Giske, J., Railsback, F., 2010. The ODD protocol: a review and first update. Ecol. Model. 221, 2760–2768. <https://doi.org/10.1016/j.ecolmodel.2010.08.019>.
- Holland, P.R., Brisbourne, A., Corr, H.F.J., McGrath, D., Purdon, K., Paden, J., Fricker, H.A., Paolo, F.S., Fleming, A.H., 2015. Oceanic and atmospheric forcing of Larsen C Ice-Shelf thinning. Cryosurgery 9, 1005–1024. <https://doi.org/10.5194/tc-9-1005-2015>.
- Jiang, J., DeAngelis, D., Teh, S., Krauss, K., Wang, H., Lie, H., Smith, T., Koh, H., 2016. Defining the next generation modeling of coastal ecotone dynamics in response to global change. Ecol. Model. 326, 168–176. <https://doi.org/10.1016/j.ecolmodel.2015.04.013>. 24 April, 2016.
- Jorgensen, S.E., 1996. Handbook of Environmental and Ecological Modeling. CRC Press, Boca Raton, FL, pp. 688 ISBN: 978-1-56670-202-7.
- Miami-Dade County Agriculture, 2019. <https://www.miamidade.gov/business/agriculture.asp>, Accessed January 3, 2019.
- McThenia, A., Martin, W., Reynolds, J., 2017. Rising tides and sinking brines: managing the threat of salt water intrusion. Florida Water Resour. J. 32–38. <https://fkaa.blob.core.windows.net/linkdocs/Managing%20the%20Threat%20of%20Salt%20Water%20Intrusion.pdf>.
- National Academies of Sciences, Engineering, and Medicine, 2018. Progress Toward Restoring the Everglades: The Seventh Biennial Review – 2018. The National Academies Press, Washington, DC. <https://doi.org/10.17226/25198>. 210 p., ISBN: 978-0-309-47978-3.
- NASA Advisory Council, Earth System Sciences Committee, 1986. Earth system science overview: a program for global change. National Aeronautics and Space Administration, Washington, D.C. pp. 50. <https://doi.org/10.17226/19210>.
- Nelder, J.A., Mead, R., 1965. A simplex algorithm for function minimization. Comput. J. 7, 308–313. <https://doi.org/10.1093/comjnl/7.4.308>.
- Park, J., Stabernau, E., Kotun, K., 2017a. Sea-level rise and inundation scenarios for national parks in South Florida. Park Sci. 33 (1), 63–73. [https://www.nps.gov/articles/parkscience33-1\\_63-73\\_park\\_et\\_el\\_3860.htm](https://www.nps.gov/articles/parkscience33-1_63-73_park_et_el_3860.htm).
- Park, J., Stabernau, E., Redwine, J., Kotun, K., 2017b. South Florida's Encroachment of the Sea and Environmental Transformation over the 21st Century. J. Mar. Sci. Eng. 5 (3), 31. <https://doi.org/10.3390/jmse50300312017>.
- Rintz, R.E., Loope, L.L., 1978. Vegetation map of Taylor Slough, Everglades National Park, Florida. U.S. National Park Service, South Florida Research Center, Report T-

566. Lyons Map Co., Miami, Florida. <http://purl.flvc.org/fcla/dt/3325304>.
- Ross, M., Meeder, J., Sah, J., Ruiz, P., Telesnicki, G., 2000. The southeast saline everglades revisited: 50 years of coastal vegetation change. *J. Veg. Sci.* 11 (1), 101–112. <http://www.jstor.org/stable/3236781>.
- Ruiz, P., Giannini, H., Prats, M., Perry, C., Foguer, M., Garcia, A., Shamblin, R., Whelan, K., Hernandez, M., 2017. The Everglades National Park and Big Cypress National Preserve Vegetation Mapping Project. Interim Report-Southeast Saline Everglades (Region 2). Everglades National Park Natural Resource Report NPS/SFCN/NRR-2017/1494. August 2017, <https://irma.nps.gov/DataStore/DownloadFile/583479>.
- Schiff, Joel L., 2011. *Cellular Automata: A Discrete View of the World*. Wiley & Sons, Inc. ISBN 9781118030639.
- Sivapalan, M., 2018. From engineering hydrology to Earth system science: milestones in the transformation of hydrologic science. *Hydrol. Earth Syst. Sci.* 22, 1665–1693.
- <https://doi.org/10.5194/hess-22-1665-2018>.
- Telis, P.A., Zhixiao, X., Zhongwei, L., Yingru, L., Conrads, P., 2015. The Everglades Depth Estimation Network (EDEN) Surface-Water Model, Version 2: U.S. Geological Survey Scientific Investigations Report 2014-5209. <https://doi.org/10.3133/sir20145209>. 42 p.
- Wilensky, U., 1999. NetLogo. Center for Connected Learning and Computer-Based Modeling. Northwestern University, Evanston, IL. <http://ccl.northwestern.edu/netlogo/>.
- Wouters, B., Martin-Espau, A., Helm, V., Flament, T., van Wessem, J.M., Ligtenberg, S.R.M., van den Broeke, M.R., Bamber, J.L., 2015. Dynamic thinning of glaciers on the Southern Antarctic Peninsula. *Science* 348 (6237), 899–903. <https://doi.org/10.1126/science.aaa5727>.